

A parabolic solar collector for harnessing solar energy in Bucaramanga, Colombia

C. L. Sandoval-Rodriguez^{1*}, A. D. Rincon-Quintero¹, C. A. Angulo-Julio¹, O. Lengerke¹, A. J. Rodriguez-Nieves¹, N. Y. Castillo-Leon¹

¹ Faculty of Natural Sciences and Engineering, Unidades Tecnológicas de Santander, Colombia

*Corresponding author E-mail: csandoval@correo.uts.edu.co

Received Nov. 3, 2023

Revised Dec. 7, 2023

Accepted Dec. 11, 2023

Abstract

In this work, a solar energy collection system based on a parabolic solar collector adjusted to the conditions and availability of energy was designed to examine this type of collection device and evaluate the energy potential when installed in an educational institution. To do this, data from the historical series of solar radiation compiled by the POWER project (Prediction of Worldwide Energy Resources) were analyzed and compared with data from the Institute of Hydrology, Meteorology and Environmental Studies in Colombia (IDEAM).

© The Author 2023.

Published by ARDA.

Keywords: Solar collector, Renewable energy resources, Bucaramanga

1. Introduction

There has been considerable development regarding renewable and alternative energies as technological advances occur worldwide. In the report "Renewable Energy World Status Report" industry trends are presented with respect to biomass, geothermal energy, hydropower, ocean energy, concentrating solar thermal energy, solar heating, and wind power [1]–[3]. China, the United States, Turkey, Morocco, Denmark, Austria, and Iceland stand out as the points of greatest energy development [4]–[6]. In the case of Colombia, research focused on alternative electrical energy, biomass, and solar through solar panels can be mentioned, however, much importance has not been given to the development of other renewable energies [7]–[9].

In this work, a study was carried out on the use of solar thermal energy using solar collectors and the possibility of using it as energy support for the facilities of an educational institution when installed in free spaces, such as the rooftop, and thus contribute to the diversification energy and self-sufficiency [10]–[12]. This is how a solar chart was made with the help of Sun Earth Tools to reflect the position of the sun with respect to the delimited area in which the solar collector will work. Likewise, solar radiation data recorded by NASA and IDEAM were used, which were characterized to determine the expected solar radiation. A parabolic solar collector was designed according to the characteristics of the institution and that would allow greater use of solar energy, considering the variation of solar radiation at different times of the day, different days of the week, and different months of the year [13]–[16].

2. Solar radiation

Solar radiation is the set of electromagnetic radiation emitted by the sun. It is generally expressed in terms of radiant exposure or irradiance (i.e., instantaneous power of solar radiation received per unit area) and it is expressed in kW/m^2 in the international system of units [17]–[19]. Likewise, irradiation is the power that falls per unit area in a specific time and the corresponding unit in the international system is kWh/m^2 . Irradiation makes it possible to calculate energy generation according to a power value that considers variations in solar radiation in the place where the device is installed. The place designated for the installation of the solar energy harnessing system is the rooftop of building B at Unidades Tecnológicas de Santander (UTS) in Bucaramanga. The geographic coordinates of this site are latitude: 7.105 and latitude: -73.1236.

2.1. Solar radiation in the UTS

Bucaramanga is a city with a temperate-dry climate in which there are two rainy seasons and two dry seasons. The sun shines about 4 hours a day in the rainy seasons, which occur in the months of March to May and from September to November. On the other hand, the sun shines between 5 and 6 hours in the dry season months (December, January, February, June, July, and August).

The POWER project provides data sets from NASA research that contain solar-related parameters for assessing and designing renewable energy systems. Table 1 shows the average solar radiation (in kWh/m^2) in the UTS for each month from 2010 to 2017. These data were derived using radiative transfer models from satellite observations obtained from the NASA Langley Research Center (LaRC) POWER Project funded through the NASA Earth Science/Applied Science Program [20]–[22]. The variation of monthly solar radiation in kWh/m^2 from 2010 to 2017 is shown in Figure 1.

Table 1. Monthly solar radiation in the UTS (kWh/m^2)

	2010	2011	2012	2013	2014	2015	2016	2017	AVG
Jan.	5.76	5.29	5.20	5.56	5.30	5.24	5.35	5.22	5.37
Feb.	5.32	5.19	5.77	5.18	5.51	5.36	5.39	5.91	5.45
Mar.	5.51	5.32	5.49	5.00	5.58	5.58	5.70	4.68	5.36
Apr.	4.78	5.01	4.88	4.88	5.16	5.03	4.59	5.13	4.93
May	5.04	4.88	5.10	4.90	5.09	5.61	4.45	4.71	4.97
Jun.	5.03	4.97	5.37	5.31	5.33	5.23	5.46	4.82	5.19
Jul.	4.85	5.30	5.57	5.56	5.84	5.56	5.46	5.60	5.47
Aug.	5.37	5.56	5.63	5.68	5.84	5.57	5.68	5.35	5.59
Sep.	5.11	5.38	5.77	5.28	5.55	5.73	5.34	5.03	5.40
Oct.	5.18	4.85	5.20	5.20	5.08	5.03	5.10	5.04	5.09
Nov.	4.51	4.29	4.84	4.90	4.87	4.47	4.35	4.63	4.61
Dec.	4.34	4.51	4.91	4.92	4.92	5.10	4.86	5.19	4.84

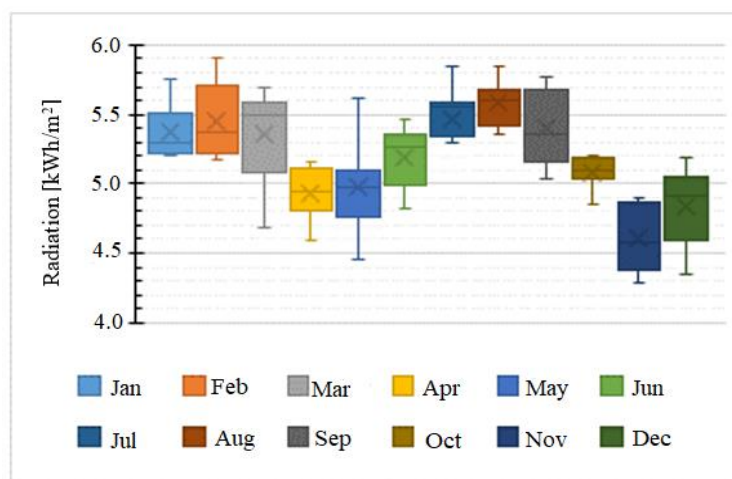


Figure 1. Monthly solar radiation variation

According to Table 1 and Figure 1, the months with the highest average solar radiation were August and July with 5.59 kWh/m^2 and 5.47 kWh/m^2 respectively. On the other hand, the month with the lowest average solar radiation was November with 4.6147 kWh/m^2 . This last data is important to establish the feasibility of the collector design [23]–[26]. Likewise, Table 2, shows the characterization of the indirect incidence per square meter over the horizontal surface in the selected place.

Table 2. Characterization of indirect incidence

	Solar radiation [kWh/m^2]	Angle of incidence (related to northeast)	Thermal units [BTU]
Jan.	5.27	$110^\circ - 119^\circ$	17 982
Feb.	5.55	98°	18 949
Mar.	5.32	$89^\circ - 97^\circ$	18 153
Apr.	4.92	$78^\circ - 86^\circ$	16 774
May	4.92	$69^\circ - 81^\circ$	16 798
Jun.	5.17	$67^\circ - 78^\circ$	17 641
Jul.	5.14	$69^\circ - 81^\circ$	17 526
Aug.	5.53	$78^\circ - 87^\circ$	18 880
Sep.	5.36	$89^\circ - 97^\circ$	18 289
Oct.	5.06	98°	17 252
Nov.	4.48	$110^\circ - 119^\circ$	15 297
Dec.	5.05	$114^\circ - 120^\circ$	17 231

The Institute of Hydrology, Meteorology and Environmental Studies of Colombia (IDEAM) has a measurement station located approximately 2 km from the UTS, specifically in the Neomundo Convention Center in Bucaramanga (Figure 2). The average solar radiation (in kWh/m^2) taken by the IDEAM at the Neomundo station for each month from 2015 to 2017 is shown in Table 3.

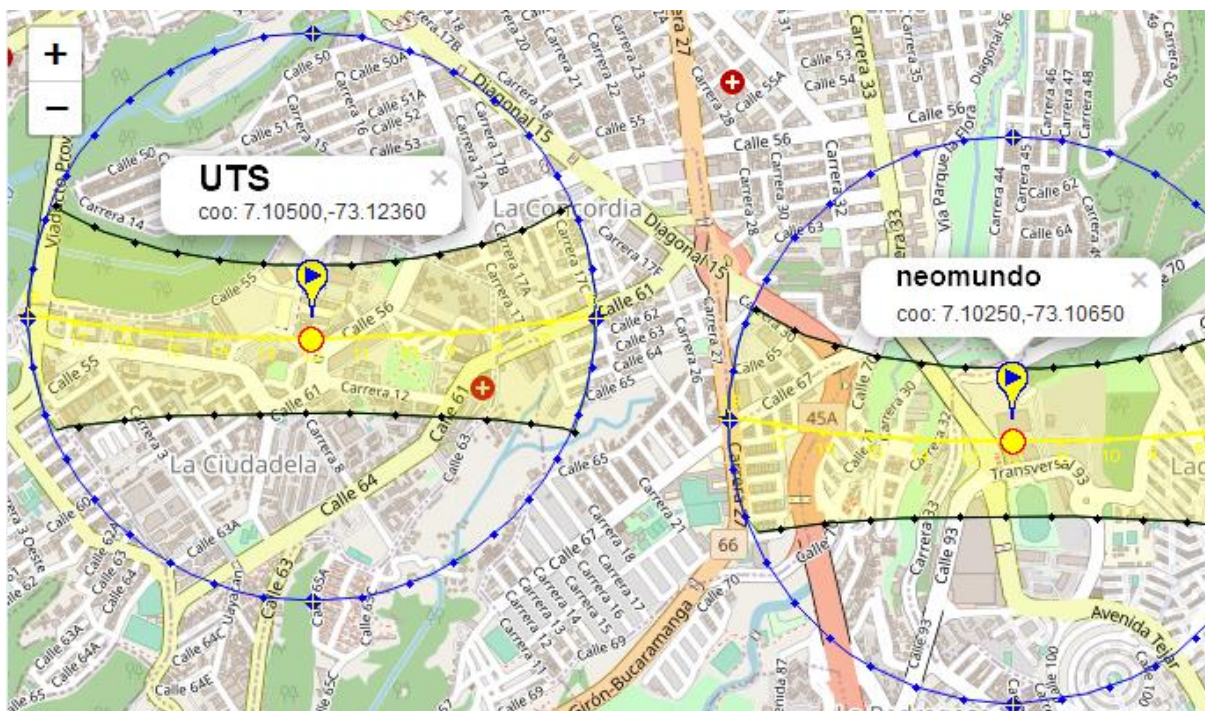


Figure 2. Neomundo measurement station location

Figure 2 shows the monthly average of the data from the POWER project and the IDEAM. The average solar radiation at both sites (UTS & Neomundo) is between 4.4 and 5.4 kWh/m^2 , with November being the month with the lowest average. To take advantage of solar energy, there are solar charts which are a graphic representation that seek to determine the position of the sun in the sky over time for a specific latitude [27]–[29]. We used the "Sun Position" tool from SunEarthTools.com to obtain the solar chart shown in Figure 4.

Table 3. Solar radiation data of the Neomundo station

	2015	2016	2017	AVG
Jan.	5.21	4.96	4.80	4.99
Feb.	5.19	4.81	5.44	5.15
Mar.	5.39	4.92	4.71	5.01
Apr.	5.23	5.03	5.36	5.21
May.	5.32	4.63	4.97	4.97
Jun.	4.60	4.95	4.78	4.78
Jul.	4.79	5.05	4.36	4.73
Aug.	4.77	5.19	5.03	5.00
Sep.	5.26	5.11	5.03	5.13
Oct.	5.30	5.10	4.85	5.08
Nov.	4.82	4.59	4.76	4.72
Dec.	4.95	4.73	4.85	4.84

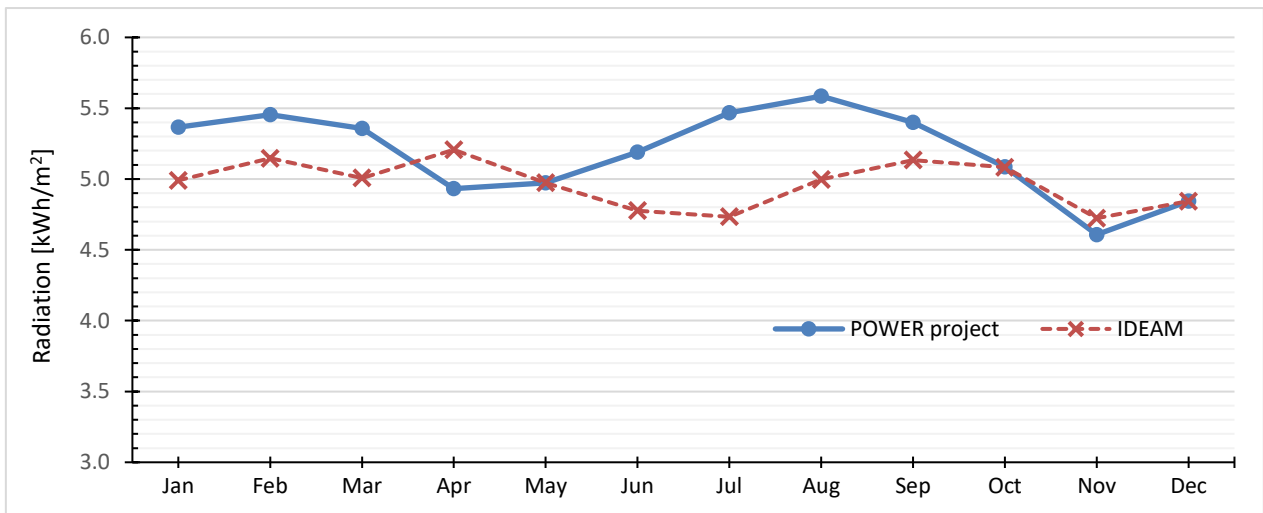


Figure 3. Average solar radiation between 2014 and 2017

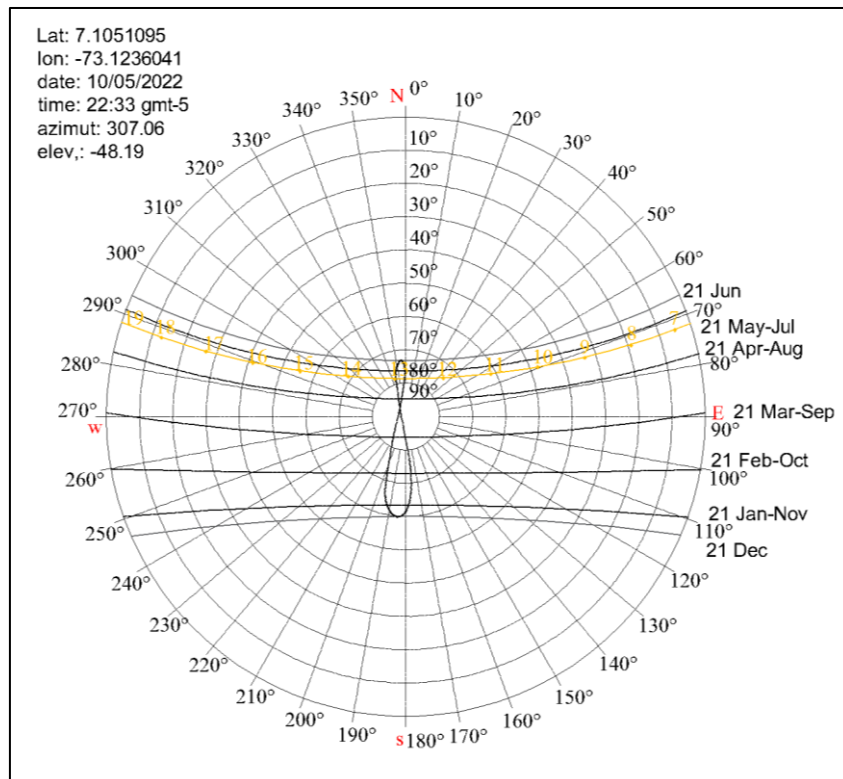


Figure 4. Solar chart for UTS location

2.2. Design of the solar collector

To obtain greater intensity per unit area, solar radiation concentrators can be used that use parabolic surfaces that concentrate the radiation at the focus of the parabola. In its design, the indirect incidence of the sun in November was used because it is the lowest average incidence in the year. A saturated water inlet temperature of 25°C and outlet temperature of 80°C, ambient temperature of 22.6°C; a heat concentration tube of 26.64 mm internal diameter through which water flows at a speed $v = 0.5$ m/s was also established. Table 4 shows the values of some properties of saturated water at the average temperature (52.5°).

Table 4. Properties of saturated water at 52.5°

Property	Value
Density	$\rho = 986.65 \text{ kg/m}^3$
Dynamic viscosity	$\mu = 525.5 \times 10^{-6} \text{ kg/m} \cdot \text{s}$
Prandtl number	$Pr = 3.4$
Thermal conductivity	$k = 0.6465 \text{ W/m} \cdot \text{°K}$

Below are some calculations relevant to collector design.

Mass flow:

$$\begin{aligned} \dot{m} &= \rho \cdot v \cdot \frac{\pi}{4} D_{int}^2 & (1) \\ \dot{m} &= 986.65 \frac{\text{kg}}{\text{m}^3} \cdot 0.5 \frac{\text{m}}{\text{s}} \cdot \frac{\pi}{4} (26.64 \times 10^{-3} \text{m})^2 \\ \dot{m} &= 0.275 \text{ kg/s} \end{aligned}$$

Reynolds number:

$$\begin{aligned} Re &= \frac{\rho \cdot v \cdot D_{int}}{\mu} & (2) \\ Re &= \frac{986.65 \cdot 0.5 \cdot 26.64 \times 10^{-3}}{525.5 \times 10^{-6}} \\ Re &= 25\,008.9 \end{aligned}$$

The length of pipe to which a turbulent fluid develops hydrodynamically and thermodynamically is given by:

$$L_h \approx L_T \approx 10 D_{int} = 0.2664 \text{m} \quad (3)$$

Nusselt number:

$$\begin{aligned} Nu &= 0.023 \cdot Re^{0.8} \cdot Pr^{0.4} & (4) \\ Nu &= 0.023 \cdot 25011.277^{0.8} \cdot 3.4^{0.4} \\ Nu &= 123.83 \end{aligned}$$

Convective heat transfer coefficient:

$$\begin{aligned} h_{int} &= Nu \cdot \frac{k}{D_{int}} & (5) \\ h_{int} &= 123.83 \cdot \frac{0.6465}{0.02664} = 3005.13 \text{ W/m}^2 \cdot \text{°K} \end{aligned}$$

Energy produced inside the tube:

$$\begin{aligned} Q_{hi} &= h_{int} \cdot Area \cdot \Delta T & (6) \\ Q_{hi} &= 3005.13 \cdot (\pi \cdot 0.02664 \cdot 0.2664) \cdot (80 - 25) \\ Q_{hi} &= 4240.64 \text{ W} \end{aligned}$$

3. Results

The design and modeling of the collector were carried out with the help of SolidWorks and Wolfram software. Figure 5 shows the base sketch of the collector's parabola made with Wolfram's "Parabolic Trough Solar Concentrator" tool, while Figure 6 show its dimensions.

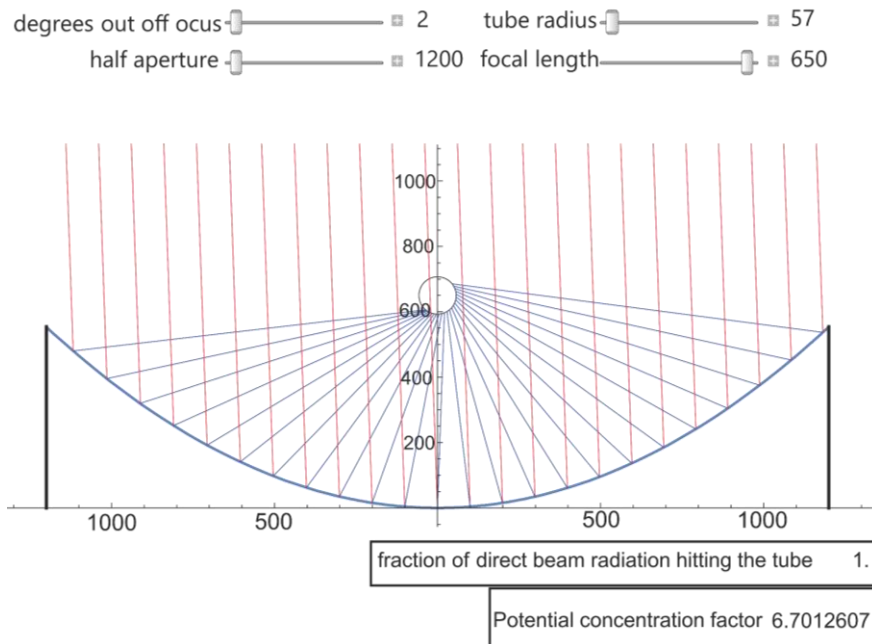


Figure 5. Parabola of the collector

Table 5 shows the results that the simulation of the parabolic solar collector yielded. With an entry angle of 2° of direct radiation, the largest area in contact with the tube is achieved, with which the radiation rectification factor or interception factor that reaches the tube is 1 [30], [31]. To the extent that this angle varies, the area of incidence in the tube will be affected and the intercept factor will decrease.

Table 5. Entry angle vs. interception factor

Entry angle	Interception factor
2°	1.0
3°	0.875
4°	0.542
5°	0.125
5.2°	0

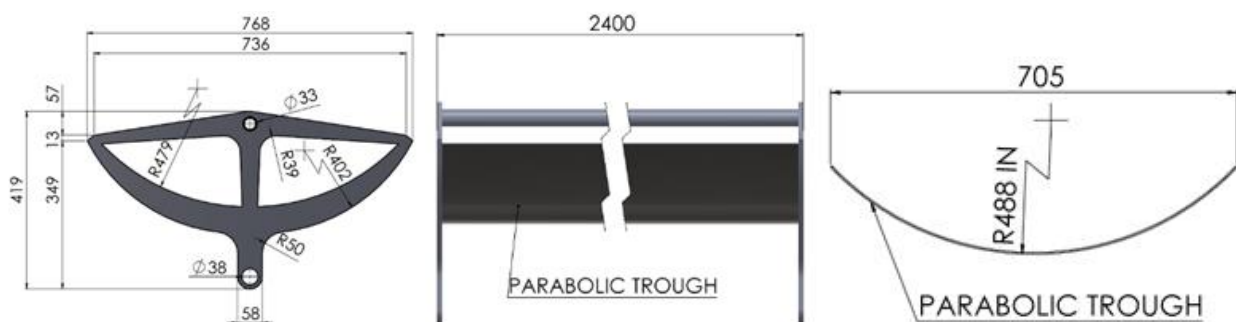


Figure 6. Collector dimensions

The 3D model of the parabolic solar collector designed is shown in Figure 7.



Figure 7. 3D model of the solar collector designed

The rooftop of building B of UTS has an approximate area of 735 m² and, due to its height, solar radiation is not hindered by the shadows of nearby buildings. Considering the dimensions of the rooftop, 24 of these collectors could be installed on it, distributed as shown in Figure 8. Taking that into account, according to the parameters used, four collectors are needed to heat the water to a temperature of 80°C [32]–[34].

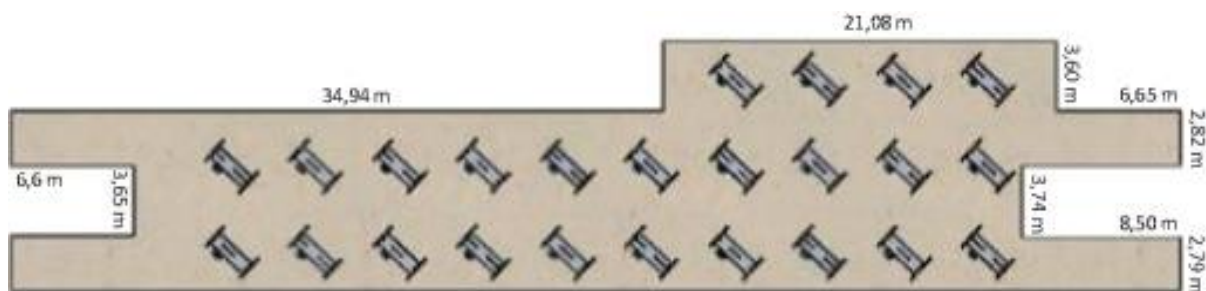


Figure 8. Distribution of solar collectors on the rooftop

4. Conclusion

The design of a parabolic solar collector has been developed that produces a total power of 4240.64 W, where the average temperature is 52.5 °C, which is high taking into account that not all of the incident energy is used. Therefore, it is recommended to evaluate the preheating situation at the entrance of the initial collector, with the objective of reducing the average temperature and determining the increase or decrease in the number of solar collectors planned for the roof of the building, which in the case of this study was 18.

Declaration of competing interest

The authors declare that they have no known financial or non-financial competing interests in any material discussed in this paper.

Funding information

This research was financially supported by Technological Units of Santander.

Acknowledgements

Special thanks to the UTS Research and Extension Directorate, led by Javier Mauricio Mendoza Paredes.

Author contribution

The contribution to the paper is as follows: C. L. Sandoval-Rodríguez, A. D. Rincon-Quintero, C. A. Angulo-Julio, O. Lengerke, A. J. Rodríguez-Nieves, N. Y. Castillo-Leon: study conception and design; C. L. Sandoval-Rodríguez, A. D. Rincon-Quintero: data collection; C. L. Sandoval-Rodríguez, A. D. Rincon-Quintero, C. A. Angulo-Julio, O. Lengerke: analysis and interpretation of results; C. L. Sandoval-Rodríguez, A. D. Rincon-Quintero: draft preparation. All authors approved the final version of the manuscript.

Ethical approval statement

Ethical approval is not applicable for this research.

Informed consent

Informed consent for the publication of personal data in this article was obtained from the participant(s).

References

- [1] P. Pourmoghadam and M. Mehrpooya, “Dynamic modeling and analysis of transient behavior of an integrated parabolic solar dish collector and thermochemical energy storage power plant,” *Journal of Energy Storage*, vol. 42, p. 103121, 2021, doi: <https://doi.org/10.1016/j.est.2021.103121>.
- [2] B. Shaker, M. Gholinia, M. Pourfallah, and D. D. Ganji, “CFD analysis of Al₂O₃-syltherm oil Nanofluid on parabolic trough solar collector with a new flange-shaped turbulator model,” *Theoretical and Applied Mechanics Letters*, p. 100323, 2022, doi: <https://doi.org/10.1016/j.taml.2022.100323>.
- [3] A. D. Rincón-Quintero *et al.*, “Manufacture of hybrid pieces using recycled R-PET, polypropylene PP and cocoa pod husks ash CPHA, by pneumatic injection controlled with LabVIEW Software and Arduino Hardware,” *IOP Conference Series: Materials Science and Engineering*, vol. 844, no. 1, 2020, doi: [10.1088/1757-899X/844/1/012054](https://doi.org/10.1088/1757-899X/844/1/012054).
- [4] G. Wang, Q. Zhu, F. Yan, and H. Chen, “Multi-model adaptive predictive control of superheated steam temperature of DSG solar parabolic-trough collector based on heat-steam ratio and its reference trajectory,” *Solar Energy*, vol. 236, pp. 393–405, 2022, doi: <https://doi.org/10.1016/j.solener.2022.03.016>.
- [5] A. Malan and K. R. Kumar, “Investigation on wind-structure interaction of large aperture parabolic trough solar collector,” *Renewable Energy*, 2022, doi: <https://doi.org/10.1016/j.renene.2022.04.141>.
- [6] L. Betancur-Arboleda, P. Hulse, K. G. Domiciano, L. Krambeck, and M. Mantelli, “Experimental study of the thermal performance of a PCM in heat sinks,” *Periodicals of Engineering and Natural Sciences*, vol. 9, no. 4, pp. 744–754, 2021, doi: [10.21533/pen.v9i4.1991](https://doi.org/10.21533/pen.v9i4.1991).
- [7] M. Deng, W. Yang, C. Chen, Z. Wu, Y. Liu, and C. Xiang, “Street-level solar radiation mapping and patterns profiling using Baidu Street View images,” *Sustainable Cities and Society*, vol. 75, no. May, p. 103289, 2021, doi: [10.1016/j.scs.2021.103289](https://doi.org/10.1016/j.scs.2021.103289).
- [8] D. Jia, L. Yang, T. Lv, W. Liu, X. Gao, and J. Zhou, “Evaluation of machine learning models for predicting daily global and diffuse solar radiation under different weather/pollution conditions,” *Renewable Energy*, vol. 187, pp. 896–906, 2022, doi: [10.1016/j.renene.2022.02.002](https://doi.org/10.1016/j.renene.2022.02.002).
- [9] B. E. Tarazona-Romero, Y. A. Muñoz-Maldonado, A. Campos-Celador, and O. Lengerke-Pérez, “Optical performance assessment of a handmade prototype of linear Fresnel concentrator,” *Periodicals of Engineering and Natural Sciences*, vol. 9, no. 4, pp. 795–811, 2021, doi: [10.21533/pen.v9i4.1987](https://doi.org/10.21533/pen.v9i4.1987).
- [10] S. Wu, R. Tang, and C. Wang, “Numerical calculation of the intercept factor for parabolic trough solar collector with secondary mirror,” *Energy*, vol. 233, p. 121175, 2021, doi: <https://doi.org/10.1016/j.energy.2021.121175>.
- [11] K. H. Almitani, A. Alzaed, A. Alahmadi, M. Sharifpur, and M. Momin, “The influence of the geometric shape of the symmetrical twisted turbulator on the performance of parabolic solar collector having hybrid nanofluid: Numerical approach using two-phase model,” *Sustainable Energy Technologies and Assessments*, vol. 51, p. 101882, 2022, doi: <https://doi.org/10.1016/j.seta.2021.101882>.

- [12] A. Joseph and S. Thomas, "A hybrid approach of surface and direct absorption of solar radiation on parabolic solar collector.," *Journal of Cleaner Production*, vol. 323, p. 129111, 2021, doi: <https://doi.org/10.1016/j.jclepro.2021.129111>.
- [13] M. S. Bükür, H. Parlamiş, M. Alwetaishi, and O. Benjeddou, "Experimental investigation on the dehumidification performance of a parabolic trough solar air collector assisted rotary desiccant system," *Case Studies in Thermal Engineering*, vol. 34, p. 102077, 2022, doi: <https://doi.org/10.1016/j.csite.2022.102077>.
- [14] A. Malekpour, R. Ahmadi, and S. Sadeghzadeh, "In situ latent thermal energy storage in underfloor heating system of building connected to the parabolic trough solar collector-an experimental study," *Journal of Energy Storage*, vol. 44, p. 103489, 2021, doi: <https://doi.org/10.1016/j.est.2021.103489>.
- [15] K. Zhao, H. Jin, Z. Gai, and H. Hong, "A thermal efficiency-enhancing strategy of parabolic trough collector systems by cascadingly applying multiple solar selective-absorbing coatings," *Applied Energy*, vol. 309, p. 118508, 2022, doi: <https://doi.org/10.1016/j.apenergy.2021.118508>.
- [16] M. A. Durán-Sarmiento, L. A. del Portillo-Valdés, Y. J. Rueda-Ordoñez, C. Borrás-Pinilla, and D. C. Dulcey-Díaz, "Modeling and simulation of a braking energy regeneration system in hydraulic hybrid vehicles in the Colombian topography," *Periodicals of Engineering and Natural Sciences*, vol. 9, no. 4, pp. 755–766, 2021, doi: 10.21533/pen.v9i4.1986.
- [17] Y. Khetib, K. Sedraoui, A. A. Melaibari, and R. Alsulami, "The numerical investigation of spherical grooves on thermal–hydraulic behavior and exergy efficiency of two-phase hybrid MWCNT-Al₂O₃/water nanofluid in a parabolic solar collector," *Sustainable Energy Technologies and Assessments*, vol. 47, p. 101530, 2021, doi: <https://doi.org/10.1016/j.seta.2021.101530>.
- [18] S. Chantasiriwan, "Solar-aided power generation in biomass power plant using direct steam generating parabolic trough collectors," *Energy Reports*, vol. 8, pp. 641–648, 2022, doi: <https://doi.org/10.1016/j.egyr.2021.11.199>.
- [19] W. N. A. Wan Roshdan, H. Jarimi, A. H. A. Al-Waeli, O. Ramadan, and K. Sopian, "Performance enhancement of double pass photovoltaic/thermal solar collector using asymmetric compound parabolic concentrator (PV/T-ACPC) for façade application in different climates," *Case Studies in Thermal Engineering*, vol. 34, p. 101998, 2022, doi: <https://doi.org/10.1016/j.csite.2022.101998>.
- [20] A. A. Alnaqi, J. Alsarraf, and A. A. A. Al-Rashed, "Numerical investigation of hydrothermal efficiency of a parabolic dish solar collector filled with oil based hybrid nanofluid," *Journal of the Taiwan Institute of Chemical Engineers*, vol. 124, pp. 238–257, 2021, doi: <https://doi.org/10.1016/j.jtice.2021.04.011>.
- [21] J. Mustafa, S. Alqaed, and M. Sharifpur, "Numerical study on performance of double-fluid parabolic trough solar collector occupied with hybrid non-Newtonian nanofluids: Investigation of effects of helical absorber tube using deep learning," *Engineering Analysis with Boundary Elements*, vol. 140, pp. 562–580, 2022, doi: <https://doi.org/10.1016/j.enganabound.2022.04.033>.
- [22] R. P. Praveen and K. V. V Chandra Mouli, "Performance enhancement of parabolic trough collector solar thermal power plants with thermal energy storage capability," *Ain Shams Engineering Journal*, vol. 13, no. 5, p. 101716, 2022, doi: <https://doi.org/10.1016/j.asej.2022.101716>.
- [23] E. Vengadesan, S. Thameenansari, E. J. Manikandan, and R. Senthil, "Experimental study on heat transfer enhancement of parabolic trough solar collector using a rectangular channel receiver," *Journal of the Taiwan Institute of Chemical Engineers*, vol. 135, p. 104361, 2022, doi: <https://doi.org/10.1016/j.jtice.2022.104361>.
- [24] A. Ranjan, Y. Dewang, J. Raghuvanshi, and V. Sharma, "Experimental evaluation of solar still coupled with parabolic trough collector," *Materials Today: Proceedings*, 2021, doi: <https://doi.org/10.1016/j.matpr.2021.11.075>.
- [25] M. Suliman, M. Ibrahim, and T. Saeed, "Improvement of efficiency and PEC of parabolic solar collector containing EG-Cu-SWCNT hybrid nanofluid using internal helical fins," *Sustainable Energy Technologies and Assessments*, vol. 52, p. 102111, 2022, doi: <https://doi.org/10.1016/j.seta.2022.102111>.

- [26] A. Abidi, “Improving the efficiency of parabolic solar collector (PSC) containing magnetic nanofluid with absorber pipe equipped with square twisted turbulator,” *Sustainable Energy Technologies and Assessments*, vol. 52, p. 102083, 2022, doi: <https://doi.org/10.1016/j.seta.2022.102083>.
- [27] R. Goyal and K. S. Reddy, “Numerical investigation of entropy generation in a solar parabolic trough collector using supercritical carbon dioxide as heat transfer fluid,” *Applied Thermal Engineering*, vol. 208, p. 118246, 2022, doi: <https://doi.org/10.1016/j.applthermaleng.2022.118246>.
- [28] R. Felsberger *et al.*, “Optical performance and alignment characterization of a parabolic trough collector using a multi-junction CPV solar cell,” *Solar Energy*, vol. 239, pp. 40–49, 2022, doi: <https://doi.org/10.1016/j.solener.2022.04.058>.
- [29] A. Abidi, A. S. El-Shafay, M. Degani, K. Guedri, S. Mohammad Sajadi, and M. Sharifpur, “Improving the thermal-hydraulic performance of parabolic solar collectors using absorber tubes equipped with perforated twisted tape containing nanofluid,” *Sustainable Energy Technologies and Assessments*, vol. 52, p. 102099, 2022, doi: <https://doi.org/10.1016/j.seta.2022.102099>.
- [30] A. Aghaei *et al.*, “Comparison of the effect of using helical strips and fines on the efficiency and thermal–hydraulic performance of parabolic solar collectors,” *Sustainable Energy Technologies and Assessments*, vol. 52, p. 102254, 2022, doi: <https://doi.org/10.1016/j.seta.2022.102254>.
- [31] B. E. T. Romero, A. C. Celador, C. L. S. Rodriguez, J. G. A. Villabona, and A. D. R. Quintero, “Design and construction of a solar tracking system for linear fresnel concentrator,” *Periodicals of Engineering and Natural Sciences*, vol. 9, no. 4, pp. 778–794, 2021, doi: 10.21533/pen.v9i4.1988.
- [32] A. D. Rincón-Quintero, L. A. Del Portillo-Valdés, A. Meneses-Jácome, J. G. Ascanio-Villabona, B. E. Tarazona-Romero, and M. A. Durán-Sarmiento, “Performance Evaluation and Effectiveness of a Solar-Biomass Hybrid Dryer for Drying Homogeneous of Cocoa Beans Using LabView Software and Arduino Hardware BT - Recent Advances in Electrical Engineering, Electronics and Energy,” in *Recent Advances in Electrical Engineering, Electronics and Energy*, M. Botto Tobar, H. Cruz, and A. Díaz Cadena, Eds., Cham: Springer International Publishing, 2021, pp. 238–252.
- [33] E. A. C. Quintana and B. E. Tarazona, “Characterization of mechanical vibrations in a metal structure using the transform Cepstrum,” *Periodicals of Engineering and Natural Sciences*, vol. 9, no. 4, pp. 767–777, 2021.
- [34] J. G. M. Lázaro and C. L. S.- Rodríguez, “Design and set up of a pulverized panela machine,” *Periodicals of Engineering and Natural Sciences*, vol. 9, no. 4, pp. 812–828, 2021.